A possible use for dimethylformamide and dimethyl sulfoxide to discern between effects of radicals and low energy electrons following irradiation of lifeforms

Birkir Reynisson

Faculty of Physical Sciences
University of Iceland
2014

A possible use for dimethylformamide and dimethyl sulfoxide to discern between effects of radicals and low energy electrons following irradiation of lifeforms

Birkir Reynisson

15 ECTS thesis submitted in partial fulfillment of a
Baccalaureus Scientiarum degree in Biochemistry

Supervisor
Oddur Ingólfsson

Co-Supervisor
Bjarni Ásgeirsson

Faculty of Physical Sciences
School of Engineering and Natural Sciences
University of Iceland
Reykjavik, June 2014

A possible use for dimethylformamide and dimethyl sulfoxide to discern between effects of radicals and low energy electrons following irradiation of lifeforms

15 ECTS thesis submitted in partial fulfillment of a B.Sc. degree in Biochemistry

Faculty of Physical Sciences
School of Engineering and Natural Sciences
University of Iceland
VRII, Hjarðarhagi 2-6
107, Reykjavik
Iceland

Telephone: 525 4000

Bibliographic information:
Birkir Reynisson, 2014, A possible use for dimethylformamide and dimethyl sulfoxide to discern between effects of radicals and low energy electrons following irradiation of lifeforms, B.Sc. thesis, Faculty of Physical Sciences, University of Iceland.

Printing: Háskólaprent, Fálkagata 2, 107 Reykjavík
Reykjavík, Iceland, June 2014

Abstract

Free radicals have been thought to be the leading cause of radiative harm to the genome. In recent years, interest has grown in the role low energy electrons play in radiative damage to DNA. In this thesis, examples are given of milestone discoveries regarding reductive DNA damage. From initial surface and gas phase experiments to the aqueous phase.

The current contribution to the field is to measure the low energy electron reactivity of two chemicals; dimethyl sulfoxide and dimethylformamide. These chemicals have shown comparable radioprotective effects in cell culture experiments. DMSO is a more potent radical scavenger than DMF but the hypothesis put forth states that DMF makes up for this with high reactivity towards low energy electrons. This is based on the molecular structure of dimethyl formamide. To test the hypothesis dissociative electron attachment experiments were performed on the two chemicals.

It was found that both chemicals showed low reactivity towards electrons with energy in the range of 0-10 eV. Six different fragments were recorded for DMSO. Most of which formed through a resonance at 5.5 eV. DMF did not fragment in the predicted manner but was found to be more reactive than DMSO as was anticipated.

Útdráttur

Stakeindir hafa verið taldar ráðandi orsök geislaskaða erfðamengis. Á síðustu árum hefur áhugi vaxið á hlutverki lágorkurafeinda í skaða sem erfðamengið hlýtur af háorkugeislun. Í þessari ritgerð eru valin dæmi tekin um tímamóta rannsóknir á sviðinu. Frá yfirborðs- og gasfasarannsóknum yfir í vatnsfasann.

Framlag rannsóknarinnar til sviðsins eru mælingar á hvarfgirni tveggja efna gagnvart lágorkurafeindum; dímetýl súlfoxíð og dímetýlformamíð. Efnin tvö hafa sýnt verjandi áhrif gegn háorkugeislun í frumurannsóknum. DMSO er hvarfgjarnari en DMF gagnvart stakeindum en hér er lögð fram sú tilgáta að DMF bætir upp þann mun með hárri hvarfgirni gagnvart lágorkurafeindum. Þessi tilgáta er byggð á sameindabyggingu Dímetýlformamíð en hún inniheldur cýanat-hóp. Reynt er á tilgátuna með tilraunum á sviði rjúfandi rafeindaálagningar.

Efnin mældust bæði með lága hvargirni gagnvart rafeindum með 0-10 eV hreyfiorku. DMSO brotnaði niður í fleiri sameindabrot en DMF. Þessi brot mynduðust helst gegnum rafómun

við 5.5 eV. Fyrir DMF mældist ekki það niðurbrot sem spáð var fyrir um en efnið sýndi þó hærri hvarfgirni en DMSO.

Contents

List of Figures

Abbreviations

AE	Appearance Energy
BDE	Bond Dissociation Energy
DEA	Dissociative Electron Attachment
DET	Dissociative Electron Transfer
DNA	Deoxyribonucleic acid
DMF	Dimethylformamide
DMSO	Dimethyl Sulfoxide
DSB	Double Strand Break
EA	Electron Affinity
EI	Electron Impact Ionization
FWHM	Full Width Half Maximum
IVR	Intramolecular Vibrational Resonance
RF	Radio Frequency
ROS	Reactive Oxygen Species
SSB	Single Strand Break
TNI	Transient Negative Ion
fs-TRLS	Femtosecond Time Resolved LASER Spectroscopy

Acknowledgements

My supervisor, professor Oddur Ingólfsson I thank for providing me with the opportunity and resources to do this assignment. His guidance in the writing process was an important experience. He also deserves acknowledgement for insisting that the topic of the assignment was in the field of biochemistry. Professor Bjarni Ásgeirsson I thank for bearing with me on this cross subject assignment.

The basement group of Raunó has taught and helped me a great deal. Baldur, Rachel, Ragesh, Ragnheiður and Stefán: Thank you all for your help with SIGMA, insightful discussions and the good times had. Special thanks go to Dr. Benedikt Ómarsson and Dr. Frímann Haukur Ómarsson. Their guidance during the summer of 2013 served as a cornerstone of this assignment and their advice is highly appreciated.

Finally I would like to thank my parents, for their patience and support.

BaRa BirRa FrOSt BeRa

1 Introduction

Cells are mostly composed of water. The properties of water are therefore interconnected with life. When water is submitted to high energy radiation (>1 MeV) each photon can cause a cascade of reactions. The photon leaves in its wake free electrons and H_2O^+ that can further dissociate and give rise to $OH^{\cdot}$.[1] Such high energy radiation has long been associated with mutation, cell death and cancer. Photons can directly interact with DNA and cause mutation but this is not thought to be the major cause of radiative cell death.[2] Rather, it is reactions of secondary particles with DNA that links radiation and cell death.

The cause of radiative mutation and cell death has mostly been attributed to reactions of $OH^{\cdot}$ since it is a known cause of damage to cells.[3] The mitochondrial free radical theory of ageing is a long standing theory that claims ageing is a result of accumulation of cellular damage traced to free radicals.[4] Reactive Oxygen Species (ROS) are a natural product of imperfect oxidative phosphorylation in the mitochondria. Such species are also the source of damage caused by many toxic metals.[5] ROS can react with cellular components (lipids, DNA, proteins) and can have lasting repercussions by mutating DNA. Oxidative damage of cells is a fact but recently interest has risen in the reductive damage of biomolecules by free electrons.

Electrons formed by radiative ionization of water quickly lose their energy through inelastic scattering and are subsequently solvated. For this reason they have in the past been mostly disregarded as a source of DNA damage. However, around the turn of the millennium subionization energy electrons were shown to react with DNA through resonances.[6] This initial discovery sparked further studies on resonant reactions of electrons with DNA components. These results make the high number of electrons stemming from photoionization highly relevant when considering mutation caused by radiation.

Dimethyl sulfoxide (DMSO) and dimethylformamide (DMF); seen in figure 1.1, have both been shown to decrease mortality in γ-irradiated cells[7, 8, 9]. In the past, this has been accounted for by the high reactivity of the compounds with $OH^{\cdot}$. DMSO is a more effective $OH^{\cdot}$ scavenger than DMF. Despite this, results of a cell mortality assay[9] indicated that the two compounds had comparable radioprotective effects. Here it is proposed that low energy electrons fill this gap in reactivity.

The working hypothesis is that DMF is highly reactive towards low energy electrons and that this property, in part, explains the radioprotectivity of the molecule. This hypothesis of high reactivity is based on the molecular structure of DMF. In DMF, the atoms N, C and O are lined up. This constellation of atoms has lead to the formation of the negative ion NCO^-; in high yields, through dissociative electron attachment of nucleobases.[10] The high electron affinity of NCO can serve as a thermochemical pull for dissociation. Once the scavenger has reacted with the electron, the resulting products are solvated and rendered harmless to DNA.

This hypothesis, that DMF is highly reactive towards low energy electrons, will be put to the test by measuring the reactivity of the two compounds towards low energy electrons via mass spectrometry. If dimethylformamide turns out to be highly reactive to low energy electrons in the gas phase, it would be indicative of high electron scavenging potency. Such scavengers can be a valuable tool in researching DNA damage because of their ability to eliminate species such as electrons allowing one to investigate the effects of remaining species. This is important when working with radiation since both radicals and electrons are formed in photoionization of water.

The experiment of this paper is in the field of Dissociative Electron Attachment. As background for the experiment a short overview is given on the theory of the field. An introduction to DNA damage is then given by tracking the process; from irradiation to DNA damage. This overview is given in the three subsequent chapters where selected examples are presented of experimental results regarding DNA damage. Firstly Dissociative Electron Attachment experiments on the components of DNA are reviewed. For comparison, the molecular mechanism behind oxidative damage of DNA is then discussed briefly. Finally, the effect of solvation on low energy electron reactions with biomolecules is covered by experimental examples. This concludes the literary review.

Turning to the experimental part of the thesis: a description of the instrumental components are provided along with how the instrument was calibrated and tuned during measurements. Experimental results are presented in the form of mass spectrometric energy spectra. Fragments of significant ion yield are discussed in relation to literature. Finally, the thesis is concluded with a short summary.

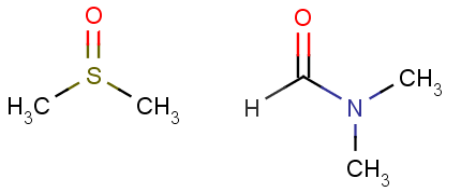

Figure 1.1: Molecular structures of dimethyl sulfoxide and dimethylformamide

2 Dissociative Electron Attachment - Theoretical Overview

Electron Impact Ionization (EI) can occur when the energy of an electron exceeds the ionizations energy of an interacting molecule. The electron loses energy in the process of ionization and also in excitation of the resulting cation. This reaction can be described by the following equation:

$$ABC + e^- \longrightarrow ABC^+ + 2e^- \tag{2.1}$$

In typical EI experiments the electron has +70 eV kinetic energy, more than enough for ionization. Molecules ionized by such electrons can be left in an excited state and, therefore, prone to further decay. This is the basis of positive mass spectra; the importance of which is described in the experimental chapter. However, the main focus of this experiment is on Dissociative Electron Attachment (DEA).

Study of Dissociative Electron Attachment entails forming a Transient Negative Ion (TNI) through attachment of subionization energy electrons and measuring the resulting anion fragments. There is considerable theory regarding the processes of formation, stabilization and reactions of the TNI. Here a short review of said theory is given as background for the following chapters and for this experiment.

2.1 Dissociative Electron Attachment

An electron approaches a molecule. If the kinetic energy of the electron is below the ionization threshold a TNI can be formed. One characteristic of such resonances is that the electron spends more time in the vicinity of the molecule than it would take for it to travel past it at constant velocity. Resonant electron attachment can result in bond rupture; dissociative electron attachment. The following equation 2.2 and figure 2.1 describe the process for a triatomic molecule ABC:

$$ABC + e^- \longrightarrow ABC^{*-} \longrightarrow AB + C^- \tag{2.2}$$

Formation of a TNI can be viewed as a vertical transition from the ground state of the neutral to the anion state in the Franck-Condon region. If the neutral molecule possesses a positive electron affinity the respective TNI formed will be in an excited state. Therefore, the ion is bound to decay. Here, a short overview is given of relevant decay channels: autodetachment and dissociation (DEA). We refer to figure 2.1 for both processes.

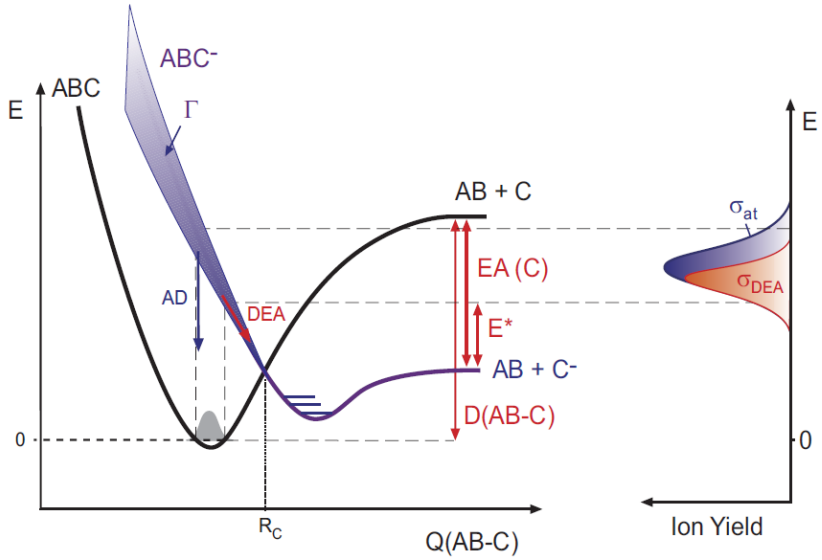

Figure 2.1: Decay channels of a TNI. The vertical axis shows energy while the horizontal one shows bond length (Q(AB-C)) for a hypothetical molecule ABC. The diagram shows a vertical transition in the Franck-Condon region from the ground state of the neutral molecule to an anionic state. Autodetachment can not occur at bond lengths exceeding R_C. Electron Affinity (EA), Excitation Energy (E^*) and bond dissociation energy (D(AB-C)) are defined in the center of the figure. To the right, attachment cross section (σ_{at}, a value signifying the efficiency of a process) of a resonant attachment is depicted. The smaller bell curve represents the DEA cross section (σ_{DEA}). The difference between the curves (blue) is lost to autodetachment. Figure from: Bald *et. al.* (2008).[11]

The process of dissociation begins immediately after the formation of the TNI if the anion state is repulsive in the Franck-Condon region. An example is if the extra electron of the TNI occupies a molecular orbital of antibonding character. On the path towards its geometrical equilibrium the bond length R in the TNI increases. While energy of the anion state is greater than of the neutral state the electron can still be ejected (Autodetachment). Once the bond length R exceeds the crossing point R_C the anion is destined for dissociation.

Most TNIs decay through autodetachment before ever reaching R_C. In the study of DEA, we measure the TNIs that cross R_C and their resulting anionic fragments. The attachment cross section; depicted on the right of figure 2.1, is the reflection of the Franck-Condon transition.

The ion yield of DEA (red in figure 2.1) is the subset of TNIs with sufficiently long lifetime with regards to autodetachment to pass R_C.

2.2 Thermochemistry

Anion formation, bond breaking and bond formation in DEA must be accounted for thermochemically. The thermochemical threshold (E_{Th}) is the minimum incident energy for a reaction to take place. It applies to DEA reactions and equation 2.3 describes how the value is calculated for reactions involving multiple bond breaks and formations. Bond Dissociation Energy (BDE) is a measure of the strength of a chemical bond, signified by D(AB-C) in figure 2.1. Electron Affinity (EA); energy released on electron addition to a neutral gas phase molecule, is also depicted in figure 2.1.

$$E_{Th} = \sum_i BDE(\text{Bonds Broken})_i - \sum_k BDE(\text{Bonds Formed})_k - EA(X) \tag{2.3}$$

In DEA experiments, anions can be measured at or above their thermochemical threshold. At subionization energy dissociation takes place through resonances. Dissociation can only take place if the resonance forms at equal to or higher energy than the thermochemical threshold. Appearance Energy (AE) of an anion is the incident electron energy at which the fragment is first spectroscopically detected. Any excess energy above the thermochemical threshold takes the form of internal (E_{Int}) and kinetic energy (E_{Kin}) of the fragments. Thus, the appearance energy can be described by the following equation.

$$E_{AE} = \sum_i BDE(\text{Bonds Broken})_i - \sum_k BDE(\text{Bonds Formed})_k - EA(X) + E_{\text{Int}} + E_{\text{Kin}} \tag{2.4}$$

2.3 Anion Formation - Resonances

Several factors contribute to the effective potential between a molecule and an electron. The diagram and equation in figure 2.2 describe this potential. The negative term of the equation is the induced dipole attraction between an electron approaching a molecule. At short range a strong repulsive potential becomes significant, explained by the Pauli exclusion principle. These two factors constitute the effective potential experienced by an electron of zero angular momentum; $l = 0$. Electrons of higher energy and angular momentum; $l \neq 0$, will encounter a centrifugal barrier to their attachment. Approaching electrons of high angular momentum

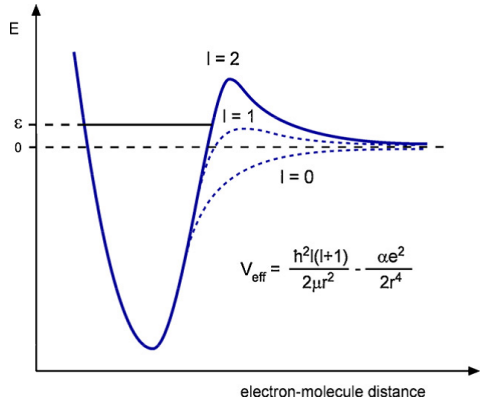

Figure 2.2: Effective potential curves of an electron approaching a molecule. The right side of the curve; relative to the minima, is described by the equation in the figure. The equation contains a repulsive centrifugal term and an attractive induced dipole term. The different lines represent potential energy barriers felt by electrons of different angular momentum. Figure from: Bald *et. al.* (2008).[11]

will feel more repulsion but they will likewise be trapped by a higher potential barrier if they manage to tunnel through. Because this electron trapping mechanism is concerned with the shape of the potential map the mechanism is generally referred to as *shape resonances*.

If the electron attachment is associated with singe particle occupancy of a previously unoccupied molecular orbital, the resonance is referred to as a *single particle shape resonance*. This nomenclature is to discern it from its more intricate counterpart: the two particle one hole, or core excited shape resonance. Such resonances form in the attachment process when the incident electron energy is sufficient to excite a *(*core) electron.

Like their single particle counterparts the core excited shape resonances lie above their respective parent state; the excited neutral state. A parent state is the molecular state formed when a TNI decays through autodetachment. In figure, 2.3 $ABCD^*$ is the parent state of both resonances.

The fact that the TNI of shape resonances is of higher energy than the parent state makes autodetachment an open channel of decay. Hence, these are termed *open channel resonances*. *Closed channel resonances* have lower energy than their parent state and, therefore, cannot decay through autodetachment. *Core excited closed channel resonances*, also known as *Feshback Resonances* are formed when a two particle-one hole resonance lies below its neutral parent state. The relative energy state of core excited resonances are depicted in figure 2.3

Intramolecular Vibrational Redistribution (IVR) is when the energy of excitation can be coupled with vibrational modes of the molecule. In IVR, the energy is *redistributed* across the molecule, thus making the TNI more stable towards autodetachment. Autodetachment

can then only take place when energy finds its way to coordinates relevant to autodetachment.

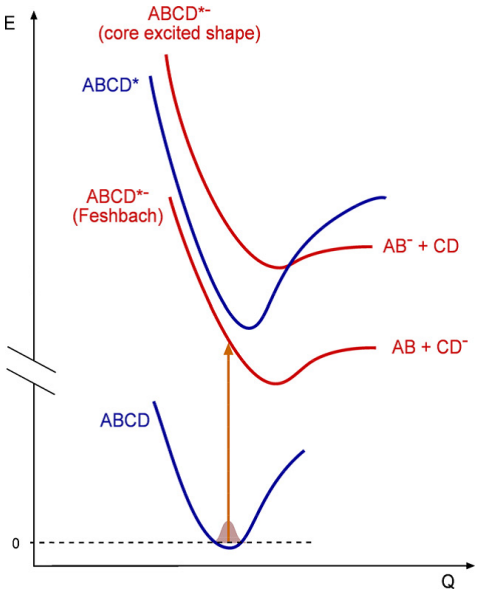

Figure 2.3: Potential energy plot showing relative energy of different core excited resonances for a hypothetical molecule ABCD. The core excited shape resonance has higher energy than its parent state, thus permitting decay by autodetachment. The Feshbach resonance has lower energy than its parent state making autodetachment a closed channel. Figure from: Bald *et. al.* (2007).[12]

3 Radiative DNA Damage

Since the early days of its discovery, exposure to radiation has been associated with illness and death. What mystified men was the biological source of this toxicity. The total energy transfer could not be to blame since a 4 Gy (Gy = J/Kg) dose that could kill a full grown man[13] is comparable to drinking a few drops of 60 $^{\circ}C$ coffee. Therefore, there must be another mechanism than radiative heating to explain the biological damage caused by radiation.

The mechanism of DNA damage caused by radiation is still a matter of debate. Direct photolytic damage to DNA has been shown to be negligible, compared to damage through secondary species formed by photolysis of water.[2] When water is irradiated, the primary absorption sets of a cascade of reactions forming radicals, electrons and excited species. In their short lifetime, these species can react with DNA causing mutagenesis or cell death. This roughly describes the multistep process of DNA damage and cell death. In an attempt to categorize the reactions based on their timescale, the process of DNA damage is generally split up into three stages, as is depicted in figure 3.1.

The physical stage describes primary absorption of the quanta and the following ionization. The timescale of this is 10^{-15}-10^{-12} seconds. High energy quanta can ionize water molecules producing electrons of high kinetic energy. These electrons can ionize water molecules through impact ionization, losing energy in the process. Electrons can further lose kinetic energy by inelastic scattering. The sum of these events is a large number of electrons of low kinetic energy formed by each photon absorbed. Calculations on the events following radiation have shown that >77% of secondary electrons have energy >20 eV.[14] Apart from electrons highly reactive radicals such as $OH^{\cdot}$ and $H^{\cdot}$ are formed. These reactions are described by the following equations.

$$H_2O + h\nu \longrightarrow H_2O^+ + e^- \tag{3.1}$$

$$H_2O^+ \longrightarrow OH^{\cdot} + H^+ \tag{3.2}$$

$$H_2O + h\nu \longrightarrow OH^{\cdot} + H^{\cdot} \tag{3.3}$$

The ratio of ionization versus homolytic cleavage is dependant on the energy quanta. UV absorption mostly results in homolytic cleavage but at higher energy the ratio tends towards ionization.[15]

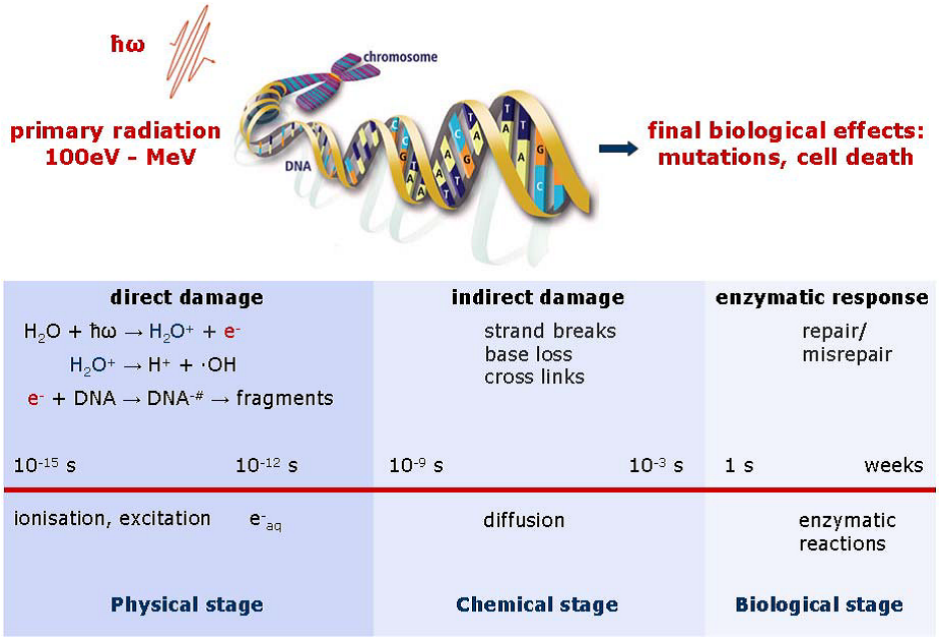

Figure 3.1: A depiction of the three stages of radiodamage: physical, chemical and biological. This cataloging is based on the timescale and thus the reactions taking place at each stage. Figure from: Bald *et. al.* (2007).[12]

The chemical stage of DNA damage describes reactions or relaxation of formed ions and radicals. These reactive species can react with DNA and cause anything from DNA strand break to base modification. Efficiency of strand breaking depends on reacting species but both $OH^{\cdot}$[16, 17, 18] and low energy electrons[19, 20] have been shown to cause strand breaks in DNA. Reactions of scavengers take place at this stage.

In the biological stage, strand breaks are repaired when possible. This happens on the timescale of seconds to days. The DNA macromolecule is a bipolymer of two complementary strands, depicted roughly in figure 3.1. Single Strand Breaks (SSB) can be repaired as DNA double strands inherently contain a negative copy to go by. Double Stranded Breaks (DSB) pose a more serious threat. Even if strands are connected successfully, nucleotides can be lost in the process. Single strand breaks in actively dividing cells are also difficult to repair since the two strands are split apart during DNA replication. Cancer and other genetic disorders have been traced to improper strand repair.[21]

4 Dissociative Electron Attachment to Biomolecules

4.1 Gas Phase Nucleobases

Some of the first evidence of DEA reactions of nucleobases were observed using instruments analogous to the apparatus used in this project.[22] Solid samples of thymine and cytosine were sublimed into a collision chamber were they interacted with low energy electrons. Parent ions were detected confirming that low energy electrons can attach to nucleobases. A wide variety of anionic fragments were observed at subionisation energy, among which were NCO^-. DEA cross section of the measured fragments were highly energy dependant, a signature of resonant reactions.

DEA experiments on nucleobases demonstrate the rich chemistry behind resonant reactions. In the case of guanine, OCN^- and CN^- are the fragments of highest DEA cross sections.[10] Such fragmentation entails aromatic ring breaking and is driven in part by the high electron affinities of OCN^- and CN^-, 3.61 eV and 3.82 eV respectively.[11] Cyanate has also been observed in the secondary fragmentation of thymine following proton loss.[23] Hydrogen/methylene substitution of N1 and N3 hydrogen; figure 4.1, experiments illustrated the bond selectivity of the reaction and indicated a reverse pericyclic reaction. These results showed that simple reactions like hydrogen abstraction can result in metastable states, pending further degradation.

Hydrogen-abstraction shows pronounced contributions in DEA experiments on nucleobases.[22] Thymine; depicted in figure 4.1, shows two contributions of H-abstraction at incident electron energy of 1.0 and 1.8 eV. There are several hydrogen atoms in thymine giving multiple options for bond breaking. Hydrogen/deuterium substitution experiments have shown remarkable bond selectivity of resonant reaction of thymine. When the methyl group of thymine is deuterated no change is observed in the $[T-H]^-$ mass spectra. No $[T-D]^-$ formation is observed. Thus, H-abstraction at subionization electron energy must stem from $N-H$ bonds.[24]

Hydrogen/methylene substitution experiments on N1 of thymine; figure 4.1, and N3 of Uracil indicated even further bond selectivity of H-abstraction.[25] Thymine and uracil have similar DEA spectra at low energy, both having $[\text{Nucleobase} - \text{H}]^-$ resonances with a narrow resonance peaking at 1.0 eV and a broader, overlapping one peaking at about 1.8 eV. Methylation of N1 in thymine suppressed a narrow resonance at 1.0 eV while N3 methylation suppressed a wider one at 1.8 eV. These observations indicate that not only do nucleobases dissociate through resonances but they do such with great bond and energy selectivity.

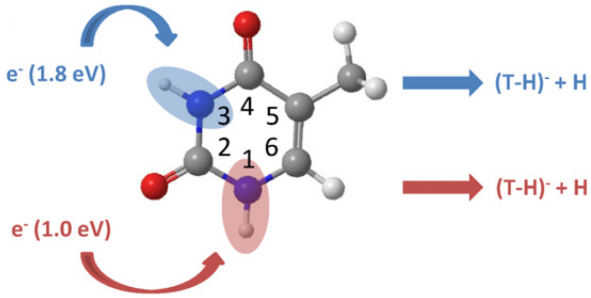

Figure 4.1: Selective H-abstraction from the thymine molecule. The figure depicts the two N−H bonds, each taking part in H-abstraction reactions at different incident electron energy. Figure from: Baccarelli *et. al.* (2011).[19]

It should not be a surprise that the simple biomolecules dissociate through subionization energy electron attachment. The abovementioned discoveries are nonetheless important milestones in proof of concept of resonant reductive damage to DNA. But salient questions remain: to what extent are these reactions of gase phase constituents transferable to DNA macromolecules? Furthermore, DNA macromolecules exist in the aquous phase *in vivo*. What effect does solvation have on resonant dissociation? Here important results in the quest to answer these questions will be presented to show the importance of resonant reductive DNA damage.

4.2 From Nucleobases to DNA

Only a few years after the first DEA experiments on nucleobases, plasmid DNA was shown to fragment when reacted with electrons of subionization energy.[6] Plasmid DNA on a metal surface, in vacuum, was irradiated with low energy electrons. Strand breaks were quantified by comparing the relative intensities of supercoiled (undamaged), circular nicked (SSB) and linear (DSB) bands on electrophoresis gels. Results indicated considerable strand breaks at sub-ionization electron energies. The breaks were dependent on electron energy. Not in a linear fashion as in photodissociation, but with definite peaks indicating resonance dissociation. Thus, it was concluded that DNA can react through DEA.

Another important observation was made. When comparing strand breaks per incident particle, low energy electrons were one to two orders of magnitude more effective than photons of comparable energy.[6] Therefore, DNA strand breaks are not only dependent on the amount of energy absorbed but also on the kind of particle that delivers said quantum of energy. These results sparked interest in research of the molecular mechanisms behind DEA to biomolecules.

4.3 Theoretical Predictions

Theoretical *ab initio* work on DNA strand break through DEA has brought insight and fruitful predictions in the field. Plasmid DNA had been shown to react through DEA at incident electron energy of >3 eV.[6] TNI formation had been observed in nucleobases at lower energy in electron transmission spectroscopy assays.[26] This TNI formation was hypothesized to form through a shape resonance by attachment to a low lying antibonding π^*-orbital. Shape resonances have low lifetime towards autodetachment but theoretical simulations provided evidence for possible dissociation despite this low lifetime.

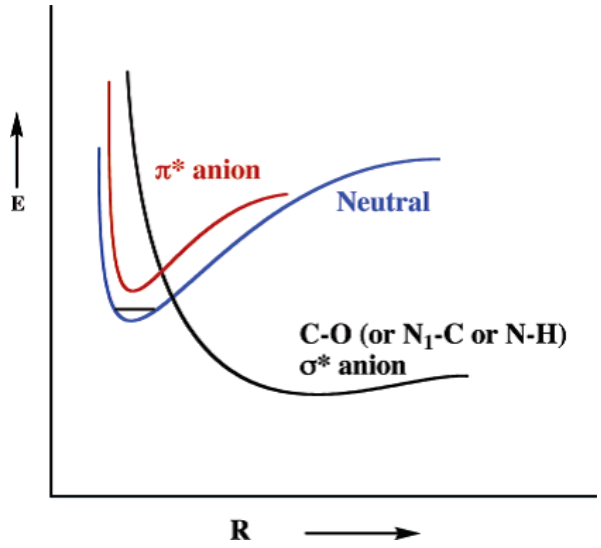

Figure 4.2: Born Oppenheimer diagram illustrating the electron transfer through conical intersection of potential energy surfaces. The transfer takes place at the nuclear coordinates at which the π^* and σ^* curves cross. Figure from: Simons *et. al.* (2006).[27]

Theoretical simulations predicted that after the electron has been attached to a π^*-orbital of nucleobase the electron is transferred to a repulsive σ^*- orbital.[28] As is depicted in figure 4.2, electron transfer is achieved through conical intersection of potential energy surfaces when π^*-anion and σ^*-anion curves cross. Electron occupancy in the repulsive σ^*-anion

state is promptly followed by dissociation. This prediction of dissociative low energy shape resonances in DNA has since been verified.[29]

Strand breaking and, thus, bond breaking takes energy. The energy gained from bond formation and electron affinity of anions formed can be an important driving force for dissociation. For example; simulations predicted the C−O bond between the phosphate and the sugar in DNA to break rapidly on account of the large electron affinity of the phosphate group.[27] Low energy electron attachment and metastable decay studies to oligonucleotides have indeed shown that the phosphate group plays a large role in stand breaks[23, 30] .

5 Oxidative DNA Damage

Here, examples are offered of the molecular mechanism behind oxidative damage to DNA. This is for the sake of comparison with reactions of subionization energy electrons.

As with resonant reactions, hydrogen abstraction is an important path in oxidative damage. Hydrogen abstraction of ribose or deoxyribose by $OH^{\cdot}$ leaves the sugar in a oxidized radical state. This species is highly reactive towards molecular oxygen, forming peroxides. Such reactions have been shown to cause strand breaks.[17]

Sugar radicals can be "saved" by glutathione in the cell. The reaction between reduced glutathione and a radical sugar causes rehydrogenation; repair of oxidative damage. The ratio of glutathione to its disulfide has been correlated with oxidative stress.[31]

Experiments with deuterated duplex DNA has shown that reactivity of different $C-H$ bonds in deoxyribose depends on their solvated surface area.[32] Reaction selectivity through solvent accessibility stems from the high reactivity of $OH^{\cdot}$. This is opposed to the selectivity of low energy electron reactions that emanates from conditions necessary for TNI formation.

Base modification is another kind of reaction caused by a $OH^{\cdot}$-radical. Such base abstractions do not pose as serious a threat to cells as strand breaks, since they can mostly be repaired enzymatically. These reactions are, nevertheless, important since their products can be used to gauge oxidative stress.[18]

Many different modified bases have been observed. Some are formed through multiple bond breaking. The first step in many of these reactions is the addition of nucleophilic $OH^{\cdot}$ to electron rich sites like double bonds. The resulting radical can then be reduced or oxidized, depending on the surroundings. If one were to distinguish between oxidative and reductive damage, the initial addition of $OH^{\cdot}$ is a key factor. Mass spectrometry has served as a powerful tool in analysing modified bases[18] and could be used in this task as well.

6 DNA Damage in Water

It has been known for over 40 years that $OH^{\cdot}$ and the hydrated electron (e^-_{hyd}) are the major radicals produced by photolysis of water.[3] A long standing paradigm was that although electrons are produced in large quantities by photoionization their contribution towards DNA damage was considered insignificant. Through ion-dipole interaction the electron reorients surrounding water molecules. This stabilizing cavity decreases the reactivity of the electron. For this reason damage to DNA following radiation has mostly been attributed to $OH^{\cdot}$.[3] Following sections are dedicated to experimental examples that show the potential prehydrated electron have to cause DNA damage

Prior to its hydration, e^-_{hyd} is a free species, e^-_{pre}. Prehydrated electrons are more reactive than their counterpart but their lifetime is on the order of fs. The lifetime of e^-_{pre} in aqueous solution has been measured with femtosecond Time Resolved laser Spectroscopy (fs-TRLS). The value measured was 500 fs.[33] This method provides an opportunity to gauge the reactivity of e^-_{pre} and thus offers a way of monitoring reactions of low energy electrons in the aqueous phase.

The following experiments were all performed using a pump-probe fs-TRLS transient absorption measurement set up. Such a set up consists of at least two lasers. One (pump) for ionizing the solvent (water, ethanol) and another (probe) for detecting the resulting ion species e.g. e^-_{pre}. By varying the delay between pump and probe by picoseconds in a series of experiments, decay and formation curves can be constructed for short lived species.

6.1 Gas Phase & Liquid Phase

CCl_4 has been extensively measured in DEA experiments. Therefore, it is a good candidate to see how the concepts of DEA transfer to the liquid phase. This was done by measuring CCl_4 solvated in ethanol by pump-probe fs-TRLS.[34] Formation/dissociation curves were constructed for both e^-_{pre} and the transient state CCl_4^{*-}. The depletion of e^-_{pre} and the formation of CCl_4^{*-} coincided completely. The time scale indicated CCl_4 is reactive towards e^-_{pre} but not its more stable counterpart e^-_{hyd}.

Figure 6.1 depicts potential curves for the ground state CCl_4, gas phase CCl_4^- and solvated CCl_4^-. The gas phase anionic potential curve crosses the ground state in the Franck-Condon region. Therefore, CCl_4 can dissociate through resonance at 0 eV incident electron energy. In polar liquid, the CCl_4^- TNI is stabilized through ion-dipole interaction. Solvation brings the CCl_4^- TNI potential curve below the parent ground state as is shown in figure 6.1.

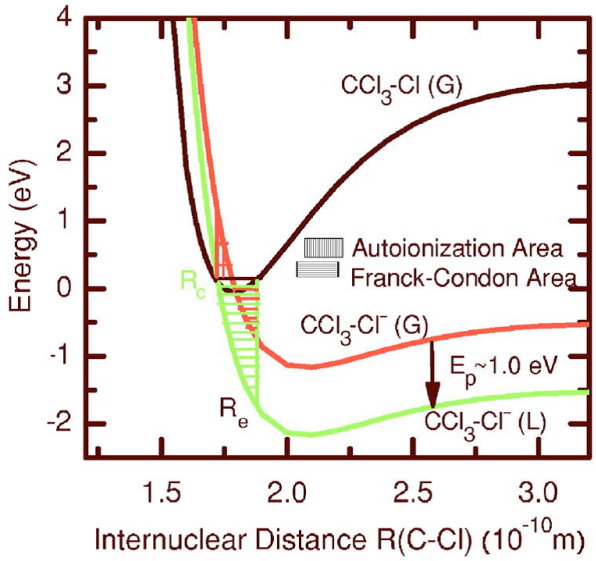

Figure 6.1: Potential energy curves for dissociation of CCl_4 in gas phase and liquid phase. The liquid phase curve (green) lies below the gas phase one on account of ion-dipole interaction with ethanol. Figure from: Wang *et. al.* (2008).[34]

The low energy of the anion curve relative to the parent state has interesting consequences. Firstly, as soon as $CCl_4{}^{-*}$ forms in the liquid phase it is committed to dissociation. The TNI potential curve lies below the parent state making each bond length R in the Franck-Condon region exceed R_C. Thus, autodetachment is a closed channel. Secondly, the DEA resonance peak shifts below 0 eV. This means loosely bound electrons such as e^-_{pre} candidates for DEA reactions.

These results indicate that the basic concepts of gas phase DEA apply to the liquid phase, with modification. The polar liquid phase stablizes the transient anion, lowering its potential curve relative to the neutral. This can make bound electrons candidates for DEA reactions. Analogous concepts have been reviewed for anion formation in clusters and other aggregate states.[35]

6.2 Dissociation of Nucleobases in Water

DEA has been measured for DNA nucleotides in aqueous media.[36] The set up was pump-probe fs-TRLS and the species measured were anions of deoxyribo nucleoside monophosphates: $dXMP^-$ (X = Adenine, Cytosine, Guanine, Thymine).

Three major observations were made for comparison of nucleotides: All nucleotides can be reduced by presolvated electrons. In support of this is the fact that each $dXMP^-$ ion was recorded within the lifetime of e^-_{pre} after laser pumping. Secondly, purines (dGMP and dAMP) were shown to be more efficient at capturing electrons than pyrimidines (dCMP and dTMP). And lastly: only dGMP and dTMP dissociate. The other two nucleotides dAMP and dCMP form stable anions.

Here gas phase and aqueous phase experiments show discrepancy. Gas phase DEA experiments[37,10] have shown all four DNA nucleobases to dissociate. A trend becomes apparent when the data from the two phases are compared: guanine and thymine are more reactive than their counterparts. In gas phase experiments, G and T dissociate into a larger variety of fragments than A and C and also with higher ion yields. It should be noted that the gas phase experiments were performed on nucleobases but not on nucleotides. Liquid phase experiments showed comparable reactivity of nucleobases, nucleoside and nucleotides towards e^-_{pre}.[36]

Thus, there is direct evidence of nucleotide dissociation in water following low energy electron attachment. Such breakdown of nucleotides can be a catalyst for further decay since one of the product still carries a charge.[23] Reactivity and proximity of the radical counterpart can also pose a threat to DNA.

6.3 Scavengers and DNA Strand Breaks

Presolvated electrons have been shown to cause strand breaks in solvated plasmid DNA. This was done by measuring the reactivity of scavengers towards e^-_{pre} and then measuring the DNA protective effects of said scavengers.[15] This experiment not only showed e^-_{pre} can cause strand breaks but that e^-_{pre} are twice as effective at it as $OH^{\cdot}$.

The reactivity of NO_3^- and DMSO, a renowned $OH^{\cdot}$ scavenger, towards e^-_{pre} was tested through pump probe fs-TRLS. This was done by ionizing water with the pump laser and monitoring the decay of e^-_{pre} with the probe laser. Results from the kinetic assays showed that both compounds were effective e^-_{pre}-scavengers. In a 2M solution of NO_3^-, electrons are quantitatively scavenged but $OH^{\cdot}$ is formed in the process, as described in equation 6.1. In

a 2M solution of DMSO, 50-54% of e^-_{pre} is scavenged. Now that the reactivity of NO_3^- and DMSO towards e^-_{pre} has been evaluated the contribution of e^-_{pre} towards DNA strand breaks can be quantified.

$$e^-_{pre} + NO_3^-(+H^+) \longrightarrow NO_3^{2-}(+H^+) \longrightarrow NO_2^- + OH^{\cdot} \tag{6.1}$$

The contribution of e^-_{pre} towards DNA strand breaks was measured through electrophoresis. Plasmid DNA samples were irradiated in the presence of different scavengers and the DNA damage quantified by comparing relative contributions of supercoiled (undamaged), SSB, and DSB on electrophoresis gels. DMSO showed the greatest photoprotective effect of all the scavengers. This is explained by its high reactivity towards both e^-_{pre} and $OH^{\cdot}$. NO_3^- is also effective at lowering strand breaks reacting with e^-_{pre} but $OH^{\cdot}$ is formed in the process, causing breaks on its own. Through comparative analysis of different scavengers it was found that the contribution of e^-_{pre} towards DNA strand breaks is twice that of $OH^{\cdot}$. These results demonstrate the large part low energy electrons play in radiative DNA damage.

7 The Instrument

All experiments of this research were performed using SIGMA. SImply a Gas Phase MAchine (SIGMA), depicted in figure 7.1, is a cross-beam gas-phase instrument equipped with a trochoidal electron monochromator, a quadrupole mass spectrometer and a channeltron ion detector. Gaseous sample is lead into a collision chamber under high vacuum where it crosses an electron beam of high energy resolution. Ionized particles are extracted into and mass selected by a quadrupole mass filter. Ions of selected mass are detected in single ion counting mode with a channeltron. Here a short description of the main components of SIGMA is provided.

7.1 Monochromator

The electron monochromator was built in house as part of the PhD work of Elías Halldór Bjarnasson. Its components and set up has been extensively described.[38] The monochromator is housed inside a vacuum chamber held under high vacuum ($\approx 10^{-8}$ mbar base pressure).

Electrons from a wolfram filament are collimated by a magnetic field and guided through lenses of differing voltage. In figure 7.1, the monochromator lenses are marked by the letter M. In the volume between lenses M5 and M6, electrons are affected simultaneously by orthogonal magnetic and electric fields. Under such conditions the electrons drift at constant speed, perpendicular to the electric and magnetic field, independent of their initial velocity. Slower electrons drift for a longer period than faster ones, shifting them further from their original straight path target on M7.[39] A narrow band of the fanned out electron beam is selected by the offset of the M7 aperture relative to the M4 one. Next, the electrons are directed to the collision chamber.

To control e^--energy in the collision chamber, the potential of M is ramped with respect to C. By referring the relative potential to a known SF_6 resonance at ≈ 0 eV, the energy scale is made absolute.

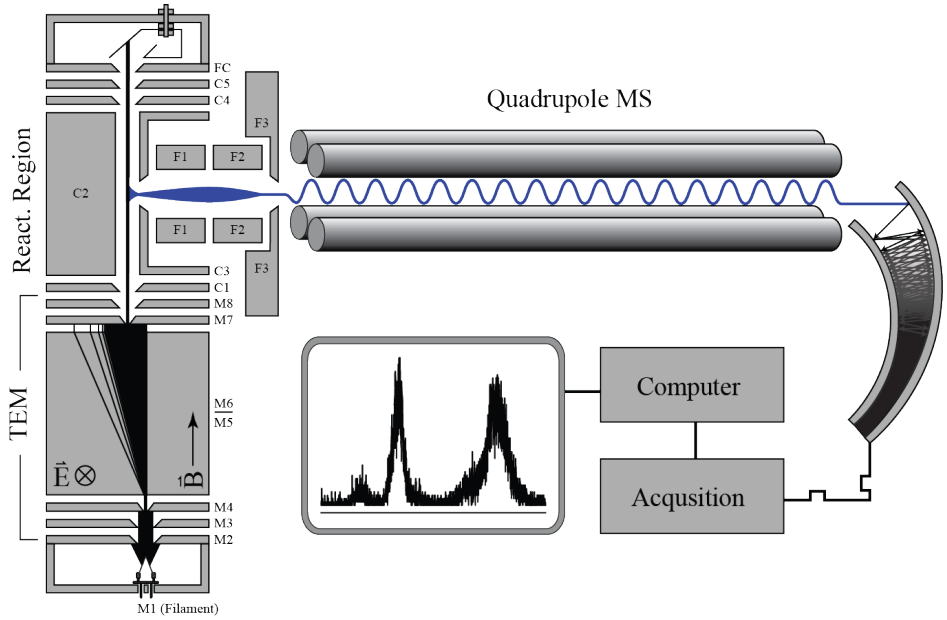

Figure 7.1: A diagram of SIGMA. The dark line shows the path of electrons through the monochromator and of ions through the quadropole. Figure from: Ómarssson (2013)[40] ©Benedikt Ómarsson.

SF_6 has been extensively researched in the field of electron attachment. The molecule is renowned for its high attachment cross section and long parent ion lifetime. The lifetime of SF_6^- anions formed through 0 eV incident electron energy is given in the range of 1 μs to >1 ms depending on instruments and conditions.[41] With such a long lifetime it follows that the natural width of $\approx$ 0 eV of SF_6 is on the order of meV. Thus, when SF_6^- is scanned around 0 eV Full Width at Half Maximum (FWHM) of the curve reflects electron energy resolution.

In this experiment, FWHM of the $SF_6{}^-$ ranged from 110 meV to about 200 meV. Possible reasons for this wide range will be discussed in the experimental chapter.

7.2 Mass Spectrometer and Detection

Charged particles formed in the collision region are extracted into the mass spectrometer by voltage difference between C2 and C3 lenses (figure 7.1). Ions travelling in the direction of the mass spectrometer are guided by Focus lenses (F) into an opening leading to the mass spectrometer. In the quadrupole, ions of a selected mass to charge ratio (m/z) retain their trajectories and arrive at the channeltron detector.

The mass spectrometer used is a HIDEN EPIC1000 quadrupole mass spectrometer (Hiden Analytical, Warrington UK). It is controlled by an Radio Frequency (RF) generator through

computer programs. The m/z range of the RF generator used is 2-1000. In most cases, the mass resolution was sufficient for our intents. Exceptions will be discussed in the results chapter. At times, resolution was lowered in an attempt to increase signal intensity. Even at these settings, the instruments resolved ions differing by only 1 amu.

8 Experiments

The instrumental set up; SIGMA, has two major controls of the experiments performed: kinetic energy of the incident electron and mass of the extracted ion. Therefore, SIGMA is capable of performing ion yield scans based on energy or based on mass.

When measuring a new compound in SIGMA, it is good practice to verify its purity and its presence in the collision chamber. This is done by a positive mass scan through electron impact ionization as described in equation 2.1. Mass of cations is scanned at constant, 70 eV electron energy. Spectra comparison of sample peaks to peaks of O_2 and N_2 indicates the partial pressure of sample in the chamber.

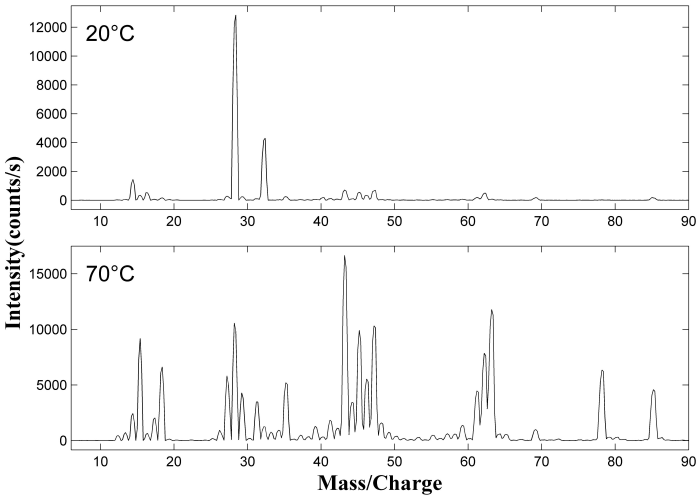

Figure 8.1: Positive ion mass spectra of DMSO impacted with 70 eV electrons. Both spectra are recorded at $\approx 1.5 \cdot 10^{-6}$ mBar. In both spectra, pronounced peaks are observed at m/z 28 and 32. They represent N_2^+ and O_2^+ respectively. The relative intensity of these signals drops considerably at higher temperature i.e. partial pressure of sample.

The first mass spectra of DMSO in figure 8.1 is dominated by N_2 and O_2 in similar ratios as in the atmosphere. This is attributed to residual gas in the inlet system. DMSO has quite low vapour pressure but its partial pressure was increased by heating the sample to 70°C. This highly improved sample to residual gas ratio as can be seen by comparing the spectra in figure 8.1.

Positive ion spectra can be used to verify the purity and presence of the sample but the aim of this experiment is to measure anion formation and fragmentation through DEA. Such experiments are performed at constant mass but the incident electron energy is varied continually over the range of interest (0-10 eV).

DMSO and DMF are polar compounds and "sticky". They have low vapour pressures and showed a tendency to condense on the surfaces of the ion optics. This problem has been encountered in other gas phase experiments on DMSO.[42] Accuracy of the monochromator suffered on account of this condensation. The best signal was achieved by calibrating the ion optics with SF_6 after DMSO or DMF had been introduced into the vacuum chamber the same day. This was the best possible effort short of introducing SF_6 into the chamber while still leaking sample into the chamber. With the current set up of the inlet system this could have overloaded the channeltron detector.

9 Results & Conclusions

9.1 Dimethyl Sulfoxide

Dimethyl Sulfoxide showed six fragments with significant ion yields. The dominant resonance was observed at $\approx$ 5.5 eV. Both S- and O-centered fragment were observed through this resonance. Spectra are presented in figures 9.1 and 9.2.

True O^- from DMSO was discerned from residual gas by varying sample temperature. At low temperature, O^- showed contributions through a wide resonance peaking at 6 eV. At higher temperature, a different $m/z = 16$ spectra was observed. A narrow peak at 5.5 eV and another at 8-10 eV appeared at the cost of the 6 eV resonance disappearing.

Atmospheric O_2 and H_2O are unavoidable contaminants in the system. Molecular oxygen has been shown to form O^- through a resonance peaking at 5.7 eV.[43] H_2O forms O^- at energy <10 eV but does so at a cross section an order of magnitude lower than O_2.[44] The resonance at 5-6 eV could therefore be from contaminants. For this reason and the fact that other fragments of DMSO peak at electron energy of $\approx$ 5.5 eV, it is deduced that the lower two spectra of figure 9.1 represent DMSO fragmentation. Similar logic can be used to deduce that contributions from OH^- do not originate from H_2O.

All sulphur containing fragments except $[\mathrm{DMSO} - \mathrm{H}]^-$ show contributions at energy of $\approx$ 5.5 eV. In a UV spectrum of DMSO,[45] an absorption peak maxing at 222 nm is attributed to a $\pi^* \longleftarrow$ n electronic excitation. A photon with a wavelength of 222 nm has energy $\approx$ 5.5 eV. This coincides with the 5.5 eV resonance observed for S-centered fragments. Thus, we tentatively assign this observed resonance to a transition associated with $\pi^* \longleftarrow n$.

A study on the translational energy distribution of photolytic fragments on DMSO found two competing reaction channels, both breaking S−C bonds.[46] It was found that the formation of SO was a sequential mechanism, loosing methylene groups in two separate events. This is in concord with our results since both CH_3SO^- and SO^- showed contributions through the same resonance.

Methyl radical formation has been measured by Electron Spin Resonance (ESR) in crys-

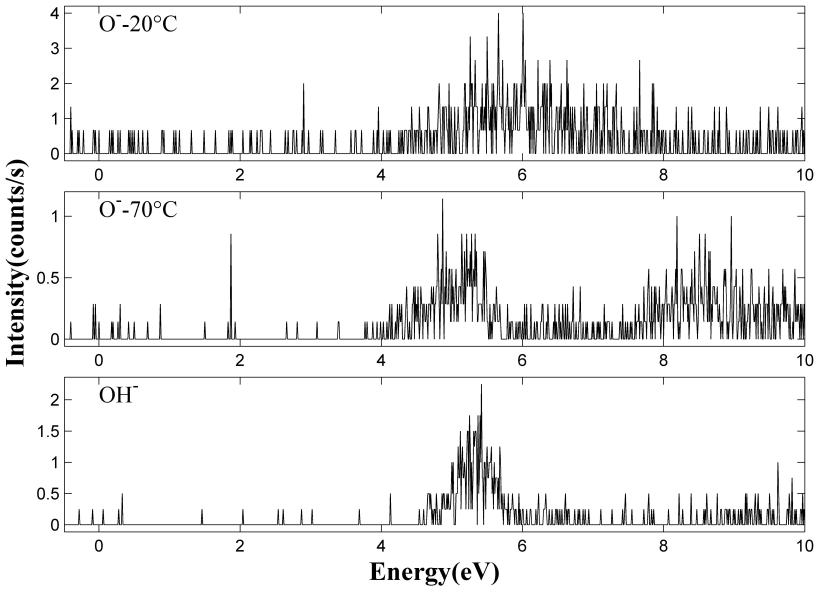

Figure 9.1: DEA spectra of oxygen centered fragments from DMSO. The top two spectra are m/z=16 fragments for DMSO at different temperature. The top spectra is attributed to contributions from molecular oxygen. The bottom two spectra have been deduced to be true contributions from DMSO.

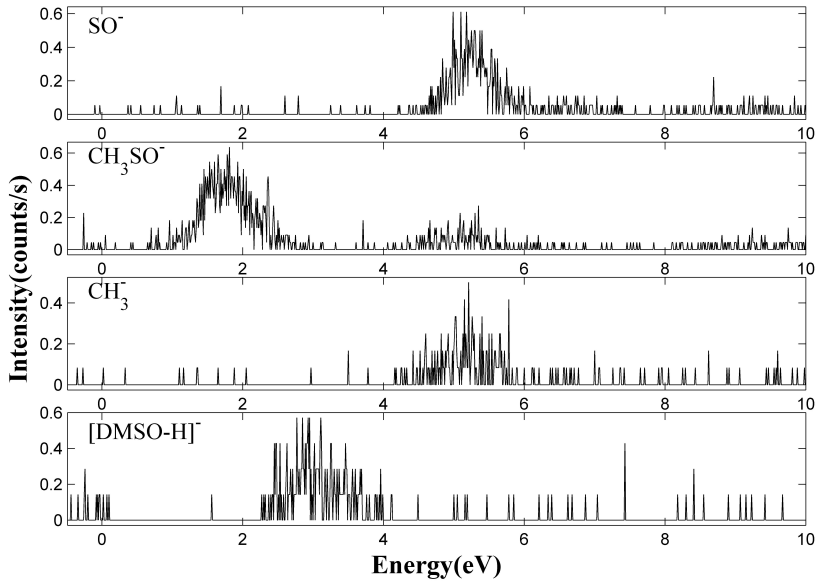

Figure 9.2: DEA spectra of sulfur centered fragments from DMSO. All fragments that form through breaking a $S-C$ bond appear through a common resonance at $\approx$ 5.5 eV.

tallized deuterated-DMSO following γ-radiation.[47] It should be noted, that ESR measures radicals so the methyl radical indicates the anion counterpart $(CH_3)SO^-$ and/or SO^-. The product is in agreement with our results and shows that DMSO can decay in similar ways in condensed phase.

Degradation of DMSO in the aqueous phase also leads to methyl radicals that eventually react to form CO_2.[48] The counter product in this reaction is methanesulfinate; formed by the addition of $OH^{\cdot}$-radical. The $OH^{\cdot}$ breakdown of DMSO is inherently different from its reactions with low energy electrons.

9.2 Dimethylformamide

Dimethylformamide showed three distinct fragments. None of which was the predicted NCO^--fragment. The most pronounced contribution observed was from m/z = 26. This could be $C_2H_2^-$; acetylene, or CN^-; cyanide, a species similar to cyanate. This problem of isobaric fragment resolution has been encountered in the DEA measurements of proline.[49] The two previously mentioned fragments formed through two resonances and were resolved using a sector field mass spectrometer. In this case CN^- was shown to form through a low lying resonance at 2 eV while $C_2H_2^-$ formed at a higher energy.

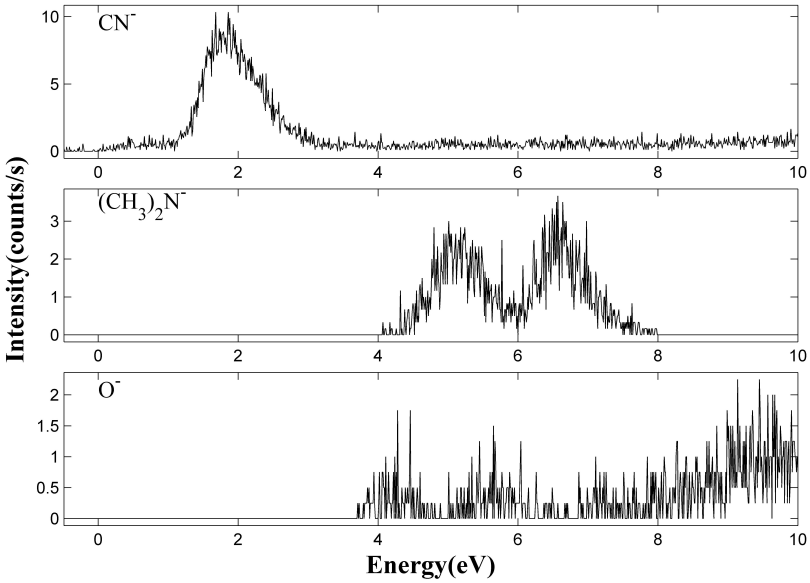

Figure 9.3: DEA spectra of fragments from DMF. The top spectrum is of CN^- formation. Of all fragments measured it has the largest ion yield. $(CH_3)_2N^-$ and O^- were recorded from 4-8 eV and from 3.5-10 eV respectively. No resonances were observed at other energy ranges under 10 eV.

Without such equipment, thermodynamic calculations are used to obtain the thermochemical thresholds of ion formation. Thermochemical thresholds were calculated at the B3LYP/ma-TZP level of theory[50, 51] using Orca 3.0 computational chemistry software.[52] The results were 1.83 eV for CN^- and 4.84 for $C_2H_2^-$. The measured low lying resonance can, therefore, not provide the energy for acetylene formation. Thus, it is concluded that the ion measured

at $m/z = 26$ is CN^-. Interestingly the energy range of the measured CN^- fragment roughly coincides with the same fragment from valine[53] and proline.[49]

The dimethylamine anion $(CH_3)_2N^-$ was detected. Its formations was observed through two close lying resonances. Only a single bond must be broken for its formation. An analogous radical fragment has been observed in liquid DMF by Electron Spin Resonance spectroscopy after exposure to UV-light.[54] Degradation was hypothesized to take place by loss of hydrogen followed by loss of CO. $[DMF - H]^-$ was not observed in our measurements. The amide bond of DMF should show double bond character, similar to the peptide bond. The peptide bond has been modelled in low energy electron experiments by acetamide.[55] Electron irradiated acetamide showed O^- formation as DMF has.

No parent ion was observed for DMF. Anionic dimers were proposed since DMF has resonance structures that both offer ways of dimerization. With an sp^3 hybridized N atom, dipole interactions could be one way of dimerization. The zwitter-ionic resonance structure of DMF could form dimers through ionic interactions. A planar cyclic dimer is improbable on account of CH_3 groups. The proposed structures; seen in figure 9.4, are resonant structures so neither truly represents DMF.

No DMF dimers were observed. This is in agreement with research on anion cluster formation of formamide, methylformamide and dimethylformamide.[56] Contrary to its simpler counterparts dimethylformamide dimer formation was not observed. This was explained by the inability of DMF to hydrogen bond with other DMF molecules. Figure 9.4 shows how N-methylformamide could form a planar dimer.

Figure 9.4: From left to right. The first two images are two resonance structures of DMF forming dimers. DMF dimers were not observed. The third structure is a possible structure of N-methylformamide dimer observed in.[56]

9.3 Conclusions

The goal of this research was to explain the molecular mechanism behind the radioprotective effects of dimethylformamide. To this end, anion fragments have been measured, caused by dissociative electron attachment of dimethylformamide and dimethyl sulfoxide. The original

hypothesis was that cyanate formation would be an effective reaction channel in DEA of DMF while DMSO would be fairly inert. This hypothesis was not confirmed by the current study. The cyanate ion was not observed. The related fragment CN^- was observed but not significantly.

The hypothesis was based on the fact that the ion had been clearly observed in DEA studies on guanine[22, 10] . The NCO^- fragment was also observed in metastable decay of thymine following hydrogen abstraction.[23]

In both nucleobase reactions, considerable bond rearrangement must take place. The thymine reaction is hypothesized to take place through reverse pericyclic reaction,[23] forming a π-bond network. There is no simple reaction mechanism to excise NCO from guanine but $[G - NCO]^-$ has been measured, indicating that the structure is relatively stable. Thus, in the cases of both nucleobases there is significant drive for the excision of NCO^-.

Here it is concluded that the cyanate ion was not observed for dimethylformamide because the molecule lacks the conjugated structure to drive the reaction. To test this counter hypothesis, dimethylpropeneamide, or further yet a unsaturated lactam (cyclic amide), could be measured in DEA experiments.

Anionic fragments resulting from DEA reactions of DMSO and DMF have been detected in low yields in this experiment. CN^- from DMF was the only fragment observed with more than a couple of counts per sec. This high reactivity of DMF relative to DMSO is in accordance with our original hypothesis but the yields are surpringly low. Absolute cross section measurements of both molecules could confirm this trend in reactivity.

DMSO has been observed to be a potent scavenger of prehydrated electrons.[15] This attribute was directly linked with the radioprotective effects of the molecule. Reaction trends towards low energy electrons, measured in the gas phase, have been shown to be qualitatively transferable to the liquid phase.[36] If this applies to DMF and DMSO and our measured reaction trends are verified, it would suggest that DMF could be an equal if not more potent e^- scavenger than DMSO. This could of course also be directly and quantitatively tested by fs-TRLS measurements described in chapter 6.

10 Summary

Low energy electrons have been approached from diverse fields. The theoretical basis of dissociative electron attachment has been discussed. Covering briefly the dynamics of TNI formation, process of dissociation and thermodynamics of DEA. An introduction was given to the processes following irradiation in the aqueous media. Thus, establishing the magnitude of low energy electrons in the aqueous media following irradiation. This was done to show the importance of considering low energy electrons in DNA damage.

Reactions of nucleobases were discussed in three different contexts. First examples were given of experiments with beams of low energy electrons. These experiments showed that both nucleobases and DNA strand can indeed react with subionization energy electrons. Furthermore, they do so with great energy and bond selectivity. An important discovery was also made with the landmark experiment of plasmid DNA: low energy electrons are more effective at causing DNA strand breaks than photons of comparable energy. Thus, resonant processes i.e. TNI formation is a potent cause of strand breaks. These results were important milestones in establishing low energy electrons as possible causes of mutagenesis.

For the sake of comparison, a short description was given of molecular mechanisms behind oxidative damage of DNA strands and nucleobases. Like low energy electrons $OH^{\cdot}$ do show selectivity in their strand breaking reaction with DNA. Their selectivity however stems from approachability of reaction sites rather than conditions for TNI formation as is the case to resonant damage.

To bring the reactions of electrons into the biologically relevant phase of solvation, examples were given of fs-TRLS experiments on e^-_{pre} reaction. Concepts of gas phase DEA still apply in the liquid phase, but with modification. Anions are stabilized through solvation and thus the anion curve is stabilized relative to the neutral ground state curve. Nucleobases were shown to be reactive with presolvated electron in the aqueous phase. Interesting discrepancies were observed between the liquid phase and gas phase DEA but reactive trends spanned across phases. Finally, the contribution of e^-_{pre} towards DNA strand break was quantified. Not only was e^-_{pre} found to cause strand breaks, but it was shown to be over doubly reactive compared to $OH^{\cdot}$.

10 Summary

Based on the structure of DMF the original hypothesis was that DMF would be highly reactive towards low energy electrons while DMSO would be relatively inert. This was proposed as a molecular mechanism for its radioprotective effects. The fragment; NCO^-, proposed as the drive for the reactivity of DMF towards low energy electron was not observed in DEA experiments. It should be noted that data presented was gathered in the face of experimental difficulties. 'Stickiness' of the compounds effected ion optics so further DEA measurements could lead to novel fragments or different trends. Still, DMF was observed to be more reactive towards low energy electrons than DMSO. To verify this reaction trend absolute cross sections of both molecules would be needed. Verification of this trend would be indicative of the high electron scavenger potency of dimethylformamide.

Bibliography

[1] **A. Allen**. *The yields of free H and OH in the irradiation of water*. Radiat. Res., 1 (1), (1954), 85.

[2] **T. Ito**, **S. Baker**, **C. Stickley**, **J. Peak** and **M. Peak**. *Dependence of the yield of strand breaks induced by γ-rays in DNA on the physical conditions of exposure: Water content and temperature*. Int. J. Rad. Biol., 63 (3), (1993), 289.

[3] **B. D. Michael** and **P. O'Neill**. *A sting in the tail of electron tracks*. Science, 287 (5458), (2000), 1603.

[4] **D. Harman**. *Ageing: a theory based on free radical and radiation chemistry*. University of California Radiation Laboratory, 1955.

[5] **M. Valko**, **C. Rhodes**, **J. Moncol**, **M. Izakovic** and **M. Mazur**. *Free radicals, metals and antioxidants in oxidative stress-induced cancer*. Chem. Biol. Interact., 160 (1), (2006), 1.

[6] **B. Bouda Ïffa**, **P. Cloutier**, **D. Hunting**, **M. A. Huels** and **L. Sanche**. *Resonant formation of DNA strand breaks by low-energy (3 to 20 eV) electrons*. Science, 287 (5458), (2000), 1658.

[7] **M. Watanabe**, **M. Suzuki**, **K. Suzuki**, **Y. Hayakawa** and **T. Miyazaki**. *Radioprotective effects of dimethyl sulfoxide in golden hamster embryo cells exposed to γ rays at 77 K: II. Protection from lethal, chromosomal, and DNA damage*. Radiat. Res., 124 (1), (1990), 73.

[8] **S. Koyama**, **S. Kodama**, **K. Suzuki**, **T. Matsumoto**, **T. Miyazaki** and **M. Watanabe**. *Radiation-induced long-lived radicals which cause mutation and transformation*. Mutat. Res. Fund. Mol. Mech. Mut., 421 (1), (1998), 45.

[9] **A. R. Kennedy** and **C. Symons**. *'Water Structure'versus 'Radical Scavenger'theories as explanations for the suppressive effects of DMSO and related compounds on radiation-induced transformation in vitro*. Carcinogenesis, 8 (5), (1987), 683.

[10] **H. Abdoul-Carime**, **J. Langer**, **M. Huels** and **E. Illenberger**. *Decomposition of purine nucleobases by very low energy electrons*. Eur. Phys. J. D., 35 (2), (2005), 399.

[11] **I. Bald**, **J. Langer**, **P. Tegeder** and **O. Ingólfsson**. *From isolated molecules through clusters and condensates to the building blocks of life*. Int. J. Mass. Spectrom., 277 (1), (2008), 4.

[12] **I. Bald**. *Low Energy Electron Induced Reactions in Gas Phase Biomolecules*. Ph.D. thesis. FB Biologie, Chemie, Pharmazie, der Freien Universität Berlin, Germany, (2007).

[13] **S. E. Pálsson**. *Líffræðileg áhrif jónandi geislunar: Lýsing og tölulegt mat*. Geislavarnir ríkisins. (2008).

[14] **S. M. Pimblott** and **J. A. LaVerne**. *Production of low-energy electrons by ionizing radiation*. Rad. Phys. Chem., 76 (8), (2007), 1244.

[15] **J. Nguyen**, **Y. Ma**, **T. Luo**, **R. G. Bristow**, **D. A. Jaffray** and **Q.-B. Lu**. *Direct observation of ultrafast-electron-transfer reactions unravels high effectiveness of reductive DNA damage*. Proc. Natl. Acad. Sci., 108 (29), (2011), 11778.

[16] **J. A. Imlay** and **S. Linn**. *DNA damage and oxygen radical toxicity*. Science, 240 (4857), (1988), 1302.

[17] **C. Chatgilialoglu** and **P. O'Neill**. *Free radicals associated with DNA damage*. Exp. Geront., 36 (9), (2001), 1459.

[18] **M. Dizdaroglu**, **P. Jaruga**, **M. Birincioglu** and **H. Rodriguez**. *Free radical-induced damage to DNA: mechanisms and measurement*. Free Radic. Biol. Med., 32 (11), (2002), 1102.

[19] **I. Baccarelli**, **I. Bald**, **F. A. Gianturco**, **E. Illenberger** and **J. Kopyra**. *Electron-induced damage of DNA and its components: experiments and theoretical models*. Phys. Rep., 508 (1), (2011), 1.

[20] **L. Sanche**. *Low energy electron-driven damage in biomolecules*. Eur. Phys. J. D., 35 (2), (2005), 367.

[21] **P. J. McKinnon** and **K. W. Caldecott**. *DNA strand break repair and human genetic disease*. Annu. Rev. Genomics Hum. Genet., 8, (2007), 37.

[22] **M. A. Huels**, **I. Hahndorf**, **E. Illenberger** and **L. Sanche**. *Resonant dissociation of DNA bases by subionization electrons*. J. Chem. Phys., 108 (4), (1998), 1309.

[23] **H. Flosadóttir**, **B. Ómarsson**, **I. Bald** and **O. Ingólfsson**. *Metastable decay of DNA components and their compositions–a perspective on the role of reactive electron scattering in radiation damage*. Eur. Phys. J. D., 66 (1), (2012), 1.

[24] **H. Abdoul-Carime**, **S. Gohlke** and **E. Illenberger**. *Site-specific dissociation of DNA bases by slow electrons at early stages of irradiation*. Phys. Rev. Lett., 92 (16), (2004), 168103.

[25] **S. Ptasinska**, **S. Denifl**, **P. Scheier**, **E. Illenberger** and **T. D. Märk**. *Bond-and Site-Selective Loss of H Atoms from Nucleobases by Very-Low-Energy Electrons (< 3 eV)*. Angew. Chem. Int. Ed., 44 (42), (2005), 6941.

[26] **K. Aflatooni**, **G. Gallup** and **P. Burrow**. *Electron attachment energies of the DNA bases*. J. Phys. Chem. A., 102 (31), (1998), 6205.

[27] **J. Simons**. *How do low-energy (0.1-2 eV) electrons cause DNA-strand breaks?* Acc. Chem. Res., 39 (10), (2006), 772.

[28] **R. Barrios**, **P. Skurski** and **J. Simons**. *Mechanism for damage to DNA by low-energy electrons*. J. Phys. Chem. B., 106 (33), (2002), 7991.

[29] **F. Martin**, **P. D. Burrow**, **Z. Cai**, **P. Cloutier**, **D. Hunting** and **L. Sanche**. *DNA strand breaks induced by 0–4 eV electrons: The role of shape resonances*. Phys. Rev. Lett., 93 (6), (2004), 068101.

[30] **Y. Zheng**, **P. Cloutier**, **D. J. Hunting**, **L. Sanche** and **J. R. Wagner**. *Chemical basis of DNA sugar-phosphate cleavage by low-energy electrons*. J. Am. Chem. Soc., 127 (47), (2005), 16592.

[31] **S. Hekimi**, **J. Lapointe** and **Y. Wen**. *Taking a "good" look at free radicals in the aging process*. Trends Cell Biol., 21 (10), (2011), 569.

[32] **B. Balasubramanian**, **W. K. Pogozelski** and **T. D. Tullius**. *DNA strand breaking by the hydroxyl radical is governed by the accessible surface areas of the hydrogen atoms of the DNA backbone*. Proc. Natl. Acad. Sci., 95 (17), (1998), 9738.

[33] **C.-R. Wang**, **T. Luo** and **Q.-B. Lu**. *On the lifetimes and physical nature of incompletely relaxed electrons in liquid water*. Phys. Chem. Chem. Phys, 10 (30), (2008), 4463.

[34] **C.-R. Wang**, **K. Drew**, **T. Luo**, **M.-J. Lu** and **Q.-B. Lu**. *Resonant dissociative electron transfer of the presolvated electron to CCl_4 in liquid: Direct observation and lifetime of the $CCl_4{}^{*-}$ transition state*. J. Chem. Phys., 128 (4), (2008), 041102.

[35] **O. Ingólfsson**, **F. Weik** and **E. Illenberger**. *The reactivity of slow electrons with molecules at different degrees of aggregation: gas phase, clusters and condensed phase*. Int. J. Mass. Spectrom., 155 (1), (1996), 1.

[36] **C.-R. Wang**, **J. Nguyen** and **Q.-B. Lu**. *Bond breaks of nucleotides by dissociative electron transfer of nonequilibrium prehydrated electrons: A new molecular mechanism for reductive DNA damage*. J. Am. Chem. Soc., 131 (32), (2009), 11320.

[37] **S. Denifl**, **S. Ptasinska**, **M. Probst**, **J. Hrušák**, **P. Scheier** and **T. Märk**. *Electron attachment to the gas-phase DNA bases cytosine and thymine*. J. Phys. Chem. A., 108 (31), (2004), 6562.

[38] **I. Bald**, **B. Ómarsson**, **m. F. H. Engman, Sarah** and **O. Ingólfsson**. *Dissociative electron attachment to titanium tetrachloride and titanium tetraisopropoxide*. Eur. Phys. J. D. DOI: 10.1140/epjd/e2014-50091-9.

[39] **A. Stamatovic** and **G. Schulz**. *Characteristics of the trochoidal electron monochromator*. Rev. Sci. Instrum., 41 (3), (1970), 423.

[40] **B. Ómarsson**. *Promoting reaction channels in dissociative electron attachment through bond formation and rearrangement*. Ph.D. thesis. Faculty of Physical Sciences, Háskóli Íslands, Iceland, (2013).

[41] **L. G. Christophorou** and **J. K. Olthoff**. *Electron attachment cross sections and negative ion states of SF_6*. Int. J. Mass. Spectrom., 205 (1), (2001), 27.

[42] **A. Hynes** and **P. Wine**. *The atmospheric chemistry of dimethylsulfoxide (DMSO) kinetics and mechanism of the OH+ DMSO reaction*. J. Atmos. Chem., 24 (1), (1996), 23.

[43] **T. Jaffke**, **M. Meinke**, **R. Hashemi**, **L. G. Christophorou** and **E. Illenberger**. *Dissociative electron attachment to singlet oxygen*. Chem. Phys. Lett., 193 (1), (1992), 62.

[44] **Y. Itikawa** and **N. Mason**. *Cross sections for electron collisions with water molecules*. J. Phys. Chem. Ref. Data., 34 (1), (2005), 1.

[45] **G. M. Thorson**, **C. M. Cheatum**, **M. J. Coffey** and **F. F. Crim**. *Photofragment energy distributions and dissociation pathways in dimethyl sulfoxide*. J. Chem. Phys., 110 (22), (1999), 10843.

[46] **D. A. Blank**, **S. W. North**, **D. Stranges**, **A. G. Suits** and **Y. T. Lee**. *Unraveling the dissociation of dimethyl sulfoxide following absorption at 193 nm*. J. Chem. Phys., 106 (2), (1997), 539.

[47] **Y. J. Chung**, **K. Nishikida** and **F. Williams**. *Methyl radical-methanesulfenate anion pairs formed by dissociative electron capture in. gamma.-irradiated crystalline dimethyl-d6 sulfoxide at 77 K.* J. Phys. Chem. A., 78 (18), (1974), 1882.

[48] **Y. Lee**, **C. Lee** and **J. Yoon**. *Kinetics and mechanisms of DMSO (dimethylsulfoxide) degradation by UV/H_2O_2 process*. Water Res., 38 (10), (2004), 2579.

[49] **P. Sulzer**, **E. Alizadeh**, **A. Mauracher**, **T. D. Märk** and **P. Scheier**. *Detailed dissociative electron attachment studies on the amino acid proline*. Int. J. Mass. Spectrom., 277 (1), (2008), 274.

[50] **A. D. Becke**. *Density-functional thermochemistry. III. The role of exact exchange*. J. Chem. Phys., 98 (7), (1993), 5648.

[51] **J. Zheng**, **X. Xu** and **D. G. Truhlar**. *Minimally augmented Karlsruhe basis sets*. Theor. Chem. Acc., 128 (3), (2010), 295.

[52] **F. Neese**. *The ORCA program system*. WIREs Comput Mol Sci, 2 (1), (2011), 73.

[53] **P. Papp**, **J. Urban**, **Š. Matejčík**, **M. Stano** and **O. Ingolfsson**. *Dissociative electron attachment to gas phase valine: A combined experimental and theoretical study*. J. Chem. Phys., 125 (20), (2006), 204301.

[54] **K. Midorikawa**, **M. Murata**, **S. Oikawa**, **S. Tada-Oikawa** and **S. Kawanishi**. *DNA damage by dimethylformamide: role of hydrogen peroxide generated during degradation*. Chem. Res. Toxicol., 13 (4), (2000), 309.

[55] **H. Abdoul-Carime**, **S. Cecchini** and **L. Sanche**. *Alteration of protein structure induced by low-energy (< 18 eV) electrons. I. The peptide and disulfide bridges*. Radiat. Res., 158 (1), (2002), 23.

[56] **C. Desfrancois**, **V. Periquet**, **S. Carles**, **J. Schermann** and **L. Adamowicz**. *Neutral and negatively-charged formamide, N-methylformamide and dimethylformamide clusters*. Chem. Phys., 239 (1), (1998), 475.